Electronic Supplementary Material (ESI) for Journal of Materials Chemistry A.

Electronic Supplementary Information for

Impact of Mg and Ti Doping in O3 Type $NaNi_{1/2}Mn_{1/2}O_2$ on Reversibility and Phase Transition During Electrochemical Na Intercalation

Kei Kubota,[a,b] Naoya Fujitani,[a] Yusuke Yoda,[a] Kazutoshi Kuroki,[a] Yusuke Tokita [a] and Shinichi Komaba *[a,b]

[a.] *Department of Applied Chemistry, Tokyo University of Science, 1-3 Kagurazaka, Shinjuku-ku, Tokyo 162-8601, Japan.*

[b.] *Elements Strategy Initiative for Catalysts and Batteries (ESICB), Kyoto University, 1-30 Goryo-Ohara, Nishikyo-ku, Kyoto 615-8245, Japan.*

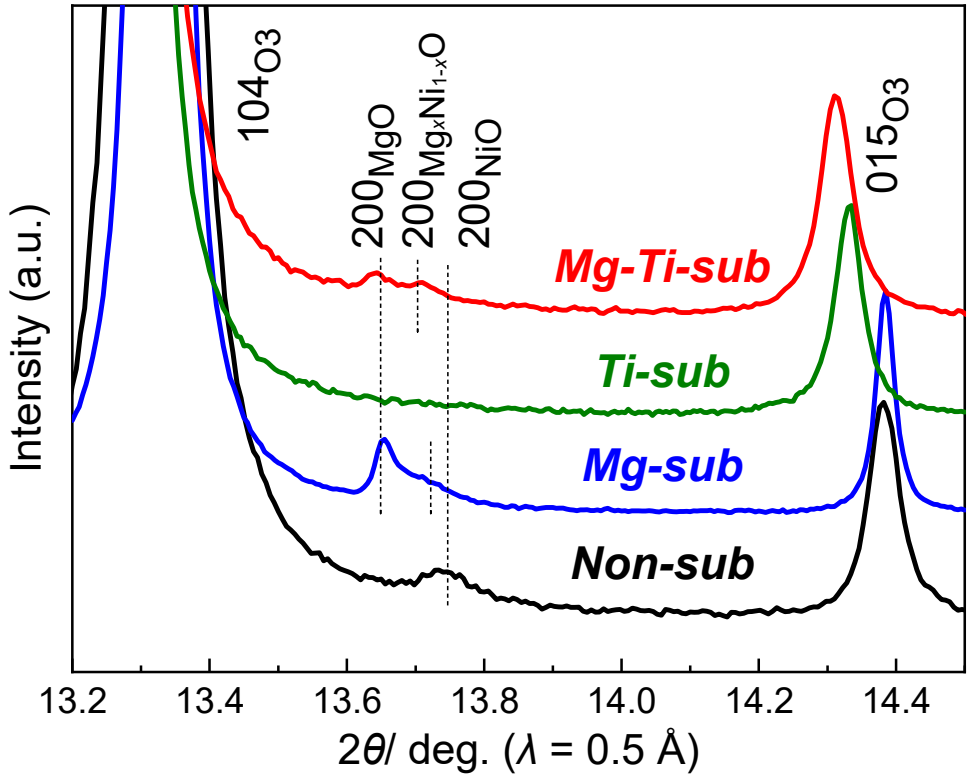

Figure S1 Magnified synchrotron powder XRD patterns of pristine $Na[Ni_{1/2}Mn_{1/2}]O_2$ (Non-sub), $Na[Ni_{4/9}Mn_{1/2}Mg_{1/18}]O_2$ (Mg-sub), $Na[Ni_{1/2}Mn_{1/3}Ti_{1/6}]O_2$ (Ti-sub), and $Na[Ni_{4/9}Mn_{1/3}Mg_{1/18}Ti_{1/6}]O_2$ (Mg-Ti-sub) in the diffraction angle range of 13.2° – 14.5°. The patterns in a wider-angle range are shown in Figure 1(a).

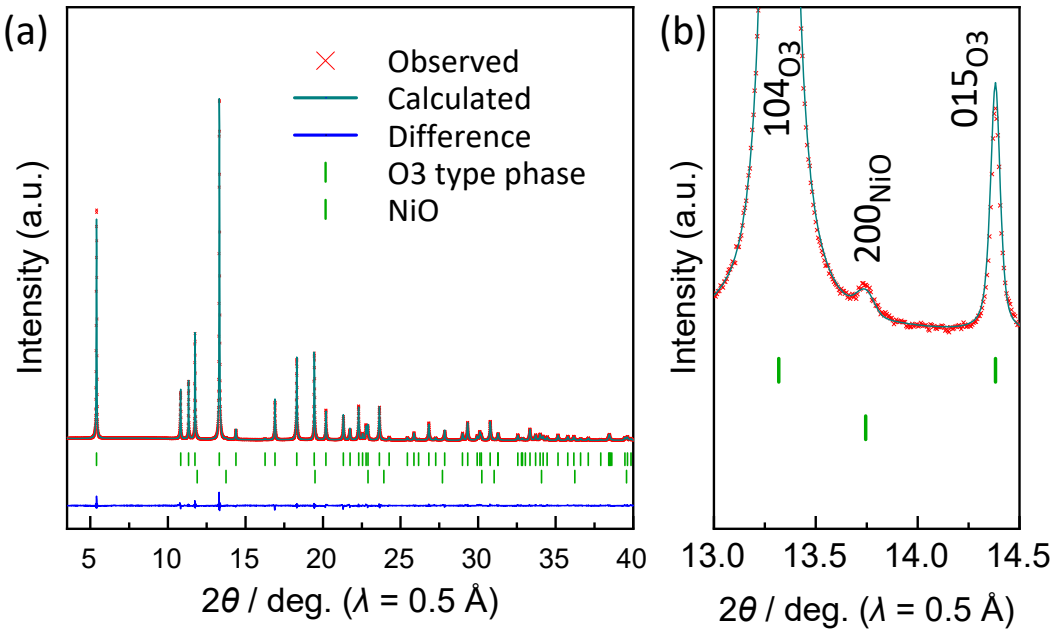

Figure S2 (a) Rietveld refinement results on the synchrotron XRD pattern of as-prepared Non-sub. (b) Magnified patterns in the diffraction angle range of 13.0° – 14.5°.

Table S1 Refined structural parameters of as-prepared Non-sub by Rietveld method on the synchrotron XRD pattern.

R_{wp} = 4.57%, R_e = 2.36%

1st phase: 99.8 mass%
Space group: $R\bar{3}m$
a = 2.96277(4) Å, c = 15.9132(2) Å, V = 120.972(3) Å^3
R_B = 0.82%, R_F = 0.65%

Atom	Wyckoff site	x	y	z	G	B / Å^2
Na	3b	0	0	1/2	0.909(2)	0.60(3)
Ni	3a	0	0	0	1/2	0.389(7)
Mn	3a	0	0	0	1/2	= B(Ni)
O	6c	0	0	0.26791(5)	1.0	0.89(2)

2nd phase: 0.2 mass%
Space group: $Fm\bar{3}m$
a = 4.1793(7) Å, V = 73.00(2) Å^3
R_B = 0.93%, R_F = 0.67%

Atom	Wyckoff site	x	y	z	G	B / Å^2
Ni	4a	0	0	0.0	1.0	0.3
O	4b	1/2	1/2	1/2	1.0	0.4

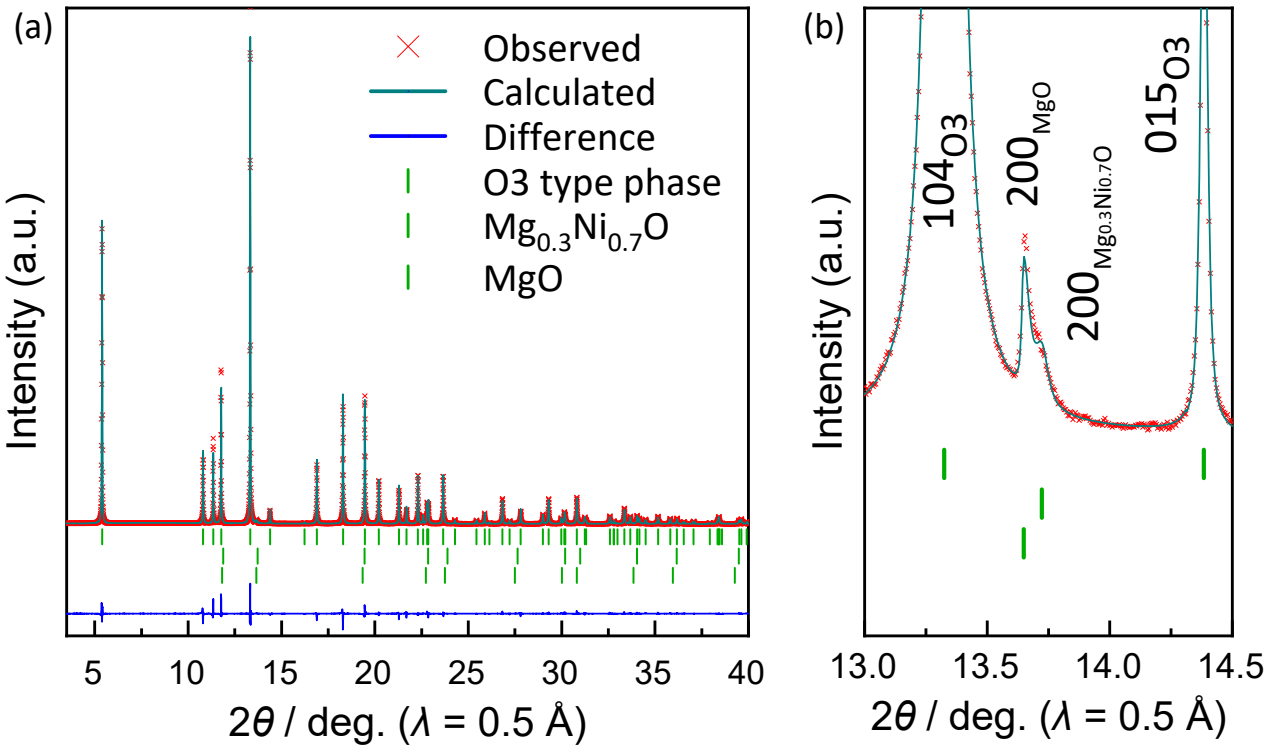

Figure S3 (a) Rietveld refinement results on the synchrotron XRD pattern of as-prepared Mg-sub. (b) Magnified patterns in the diffraction angle range of 13.0° – 14.5°.

Table S2 Refined structural parameters of as-prepared Mg-sub by Rietveld method on the synchrotron XRD pattern.

R_{wp} = 6.50%, R_e = 1.88%

1st phase: 98.77 mass%
Space group: $R\bar{3}m$
a = 2.95958(2) Å, c = 15.94768(8) Å, V = 120.9731(12) Å^3
R_B = 1.50%, R_F = 0.98%

Atom	Wyckoff site	x	y	z	g	B / Å^2
Na	3b	0	0	1/2	0.890(2)	0.75(2)
Ni	3a	0	0	0	4/9	0.354(6)
Mn	3a	0	0	0	1/2	= B(Ni)
Mg	3a	0	0	0	1/18	= B(Ni)
O	6c	0	0	0.26836(5)	1.0	0.99(2)

2nd phase: 0.78 mass%
Space group: $Fm\bar{3}m$
a = 4.1873(6) Å, V = 73.420(18) Å^3
R_B = 1.31%, R_F = 0.89%

Atom	Wyckoff site	x	y	z	g	B / Å^2
Mg	4a	0	0	0.0	0.69(11)	0.3
Ni	4a	0	0	0.0	= 1- g(Mg)	0.3
O	4b	1/2	1/2	1/2	1.0	0.4

3rd phase: 0.45 mass%
Space group: $Fm\bar{3}m$
a = 4.2099(2) Å, V = 74.613(7) Å^3
R_B = 1.31%, R_F = 0.43%

Atom	Wyckoff site	x	y	z	g	B / Å^2
Mg	4a	0	0	0.0	1.0	0.3
O	4b	1/2	1/2	1/2	1.0	0.4

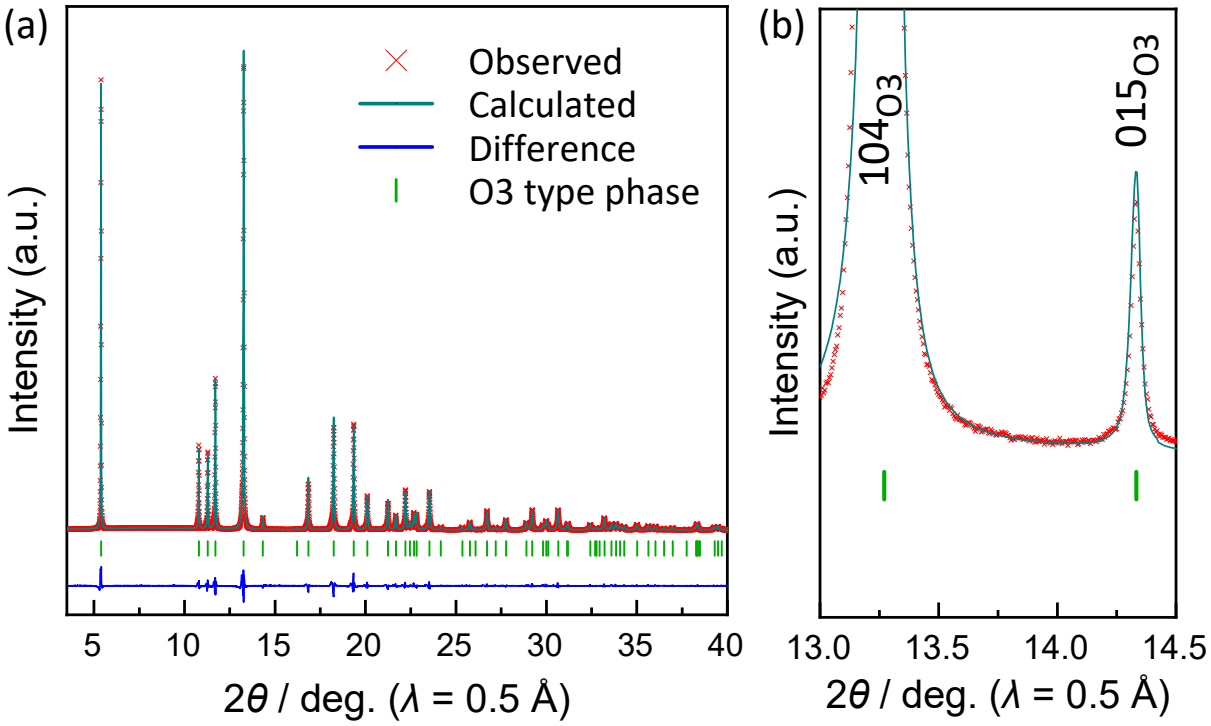

Figure S4 (a) Rietveld refinement results on the synchrotron XRD pattern of as-prepared Ti-sub. (b) Magnified patterns in the diffraction angle range of 13.0° – 14.5°.

Table S3 Refined structural parameters of as-prepared Ti-sub by Rietveld method on the synchrotron XRD pattern.

R_{wp} = 8.35%, R_e = 2.12%
Space group: $R\bar{3}m$
a = 2.97512(3) Å, c = 15.95640(11) Å, V = 122.314(2) Å
R_B = 1.06%, R_F = 0.68%

Atom	Wyckoff site	x	y	z	g	B / Å^2
Na	3b	0	0	1/2	0.922(3)	0.53(3)
Ni	3a	0	0	0	1/2	0.354(10)
Mn	3a	0	0	0	1/3	= B(Ni)
Ti	3a	0	0	0	1/6	= B(Ni)
O	6c	0	0	0.26758(7)	1.0	0.81(3)

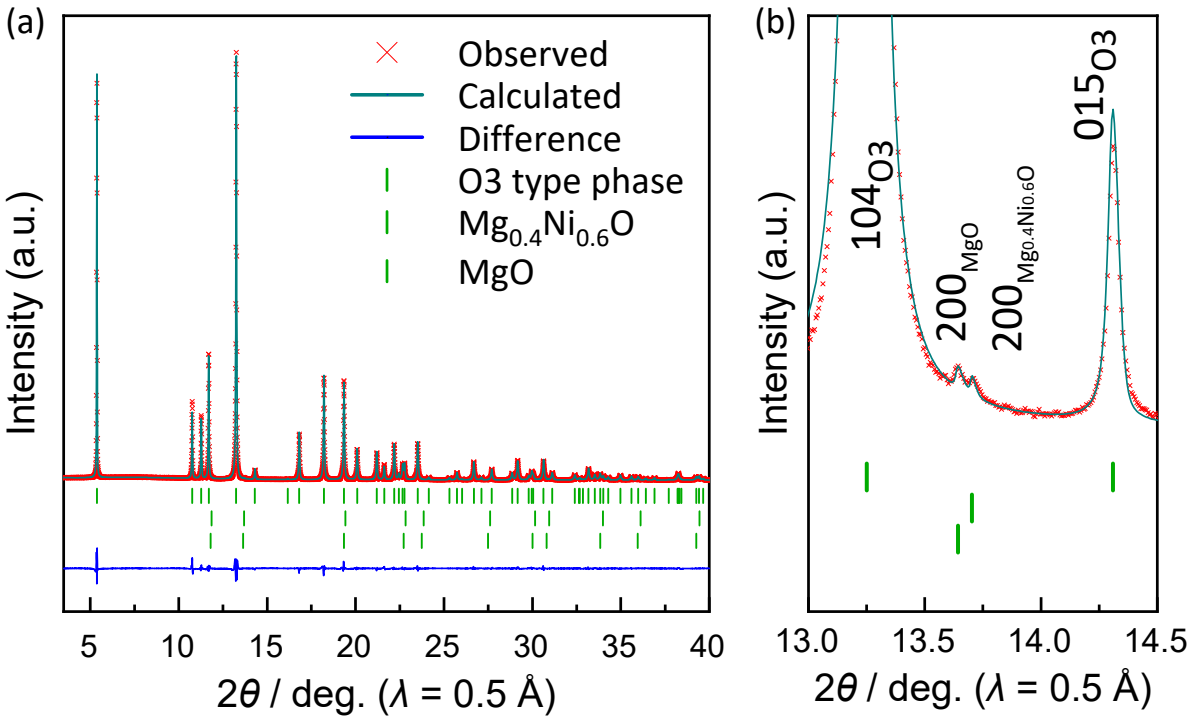

Figure S5 Rietveld refinement results on the synchrotron XRD pattern of as-prepared Mg-Ti-sub. (b) Magnified patterns in the diffraction angle range of 13.0° – 14.5°.

Table S4 Refined structural parameters of as-prepared Mg-Ti-sub by Rietveld method on the synchrotron XRD pattern.

R_{wp} = 6.02%, R_e = 1.63%

1st phase: 99.77 mass%
Space group: $R\bar{3}m$
a = 2.97587(4) Å, c = 15.9922(2) Å, V = 122.649(3) Å^3
R_B = 0.74%, R_F = 0.56%

Atom	Wyckoff site	*x*	*y*	*z*	*g*	*B* / Å^2
Na	3b	0	0	1/2	0.910(2)	0.61(3)
Ni	3a	0	0	0	4/9	0.33(1)
Mn	3a	0	0	0	1/3	= *B*(Ni)
Mg	3a	0	0	0	1/18	= *B*(Ni)
Ti	3a	0	0	0	1/6	= *B*(Ni)
O	6c	0	0	0.26771(6)	1.0	0.87(2)

2nd phase: 0.17 mass%
Space group: $Fm\bar{3}m$
a = 4.190(1) Å, V = 73.57(3) Å^3
R_B = 1.04%, R_F = 0.60%

Atom	Wyckoff site	*x*	*y*	*z*	*g*	*B* / Å^2
Mg	4a	0	0	0.0	0.4	0.3
Ni	4a	0	0	0.0	0.6	0.3
O	4b	1/2	1/2	1/2	1.0	0.4

3rd phase: 0.06 mass%
Space group: $Fm\bar{3}m$
a = 4.209(1) Å, V = 74.54(4) Å^3
R_B = 0.87%, R_F = 0.48%

Atom	Wyckoff site	*x*	*y*	*z*	*g*	*B* / Å^2
Mg	4a	0	0	0.0	1.0	0.3
O	4b	1/2	1/2	1/2	1.0	0.4

Table S5 ICP-AES results for as-prepared $Na[Ni_{1/2-x}Mn_{1/2-y}Mg_xTi_y]O_2$ samples.

Sample name	Targeted composition	Molar elemental ratio determined by ICP-AES				
		Na	Ni	Mn	Mg	Ti
Non-sub	$Na[Ni_{0.5}Mn_{0.5}]O_2$	1.04	0.48	0.52	-	-
Mg-sub	$Na[Ni_{0.44}Mn_{0.5}Mg_{0.06}]O_2$	1.06	0.44	0.52	0.04	-
Ti-sub	$Na[Ni_{0.5}Mn_{0.33}Ti_{0.17}]O_2$	1.09	0.50	0.34	-	0.16
Mg-Ti-sub	$Na[Ni_{0.44}Mn_{0.33}Mg_{0.06}Ti_{017}]O_2$	1.09	0.45	0.36	0.03	0.17

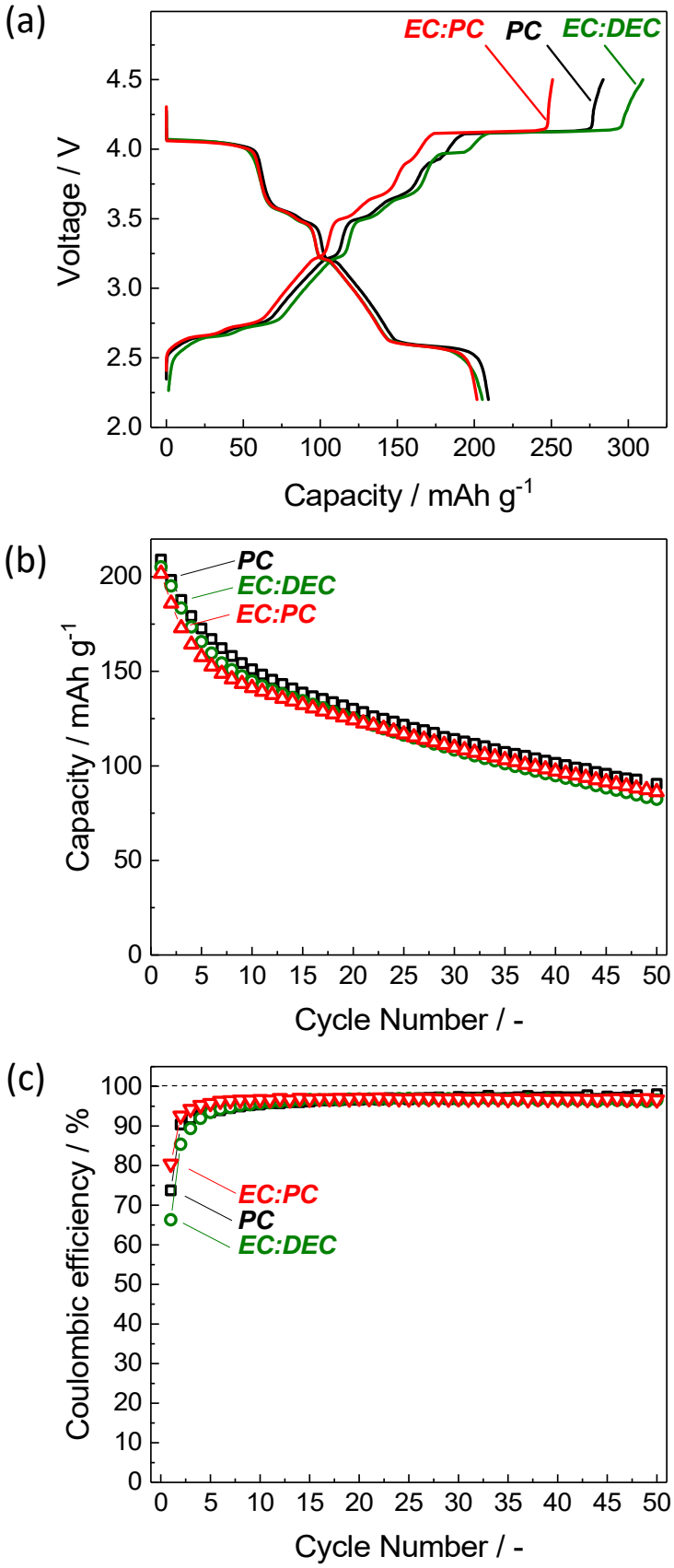

Figure S6 Electrolyte solvent dependency: (a) initial charge-discharge curves and (b) discharge capacities and (c) Coulombic efficiencies of Non-sub electrodes in non-aqueous Na cells filled with 1.0 mol dm^{-3} $NaPF_6$ dissolved in EC:DEC (1:1 v/v), EC:PC (1:1 v/v), or PC.

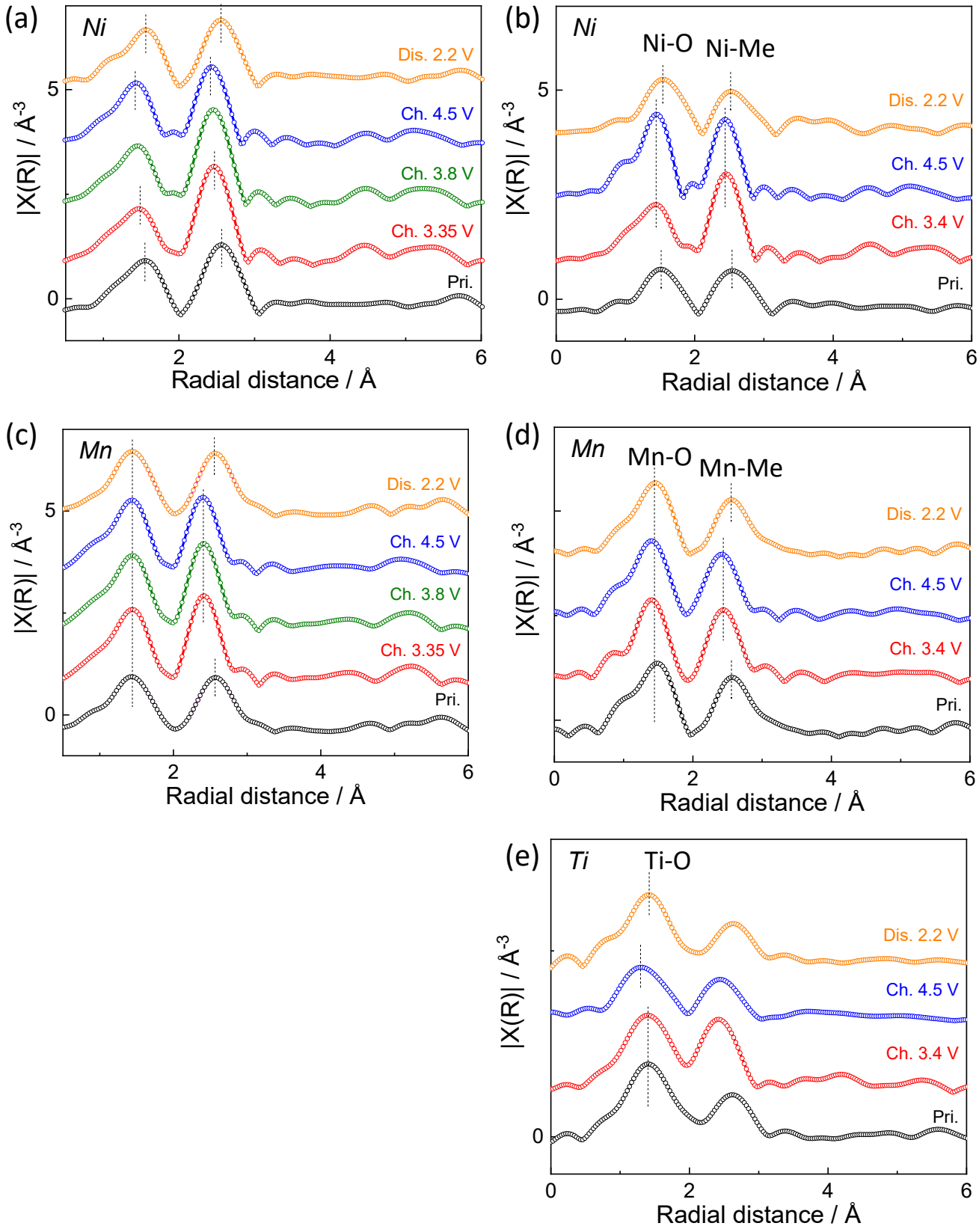

Figure S7 *Ex situ* Fourier-transformed (a, b) Ni K-edge, (c, d) Mn K-edge, and (e) Ti K-edge EXAFS spectra of (a, c) Non-sub and (b, d, e) Mg-Ti-sub electrodes. The tested electrodes were prepared by charging and discharging in Na cells followed by taking the electrodes from the cells.

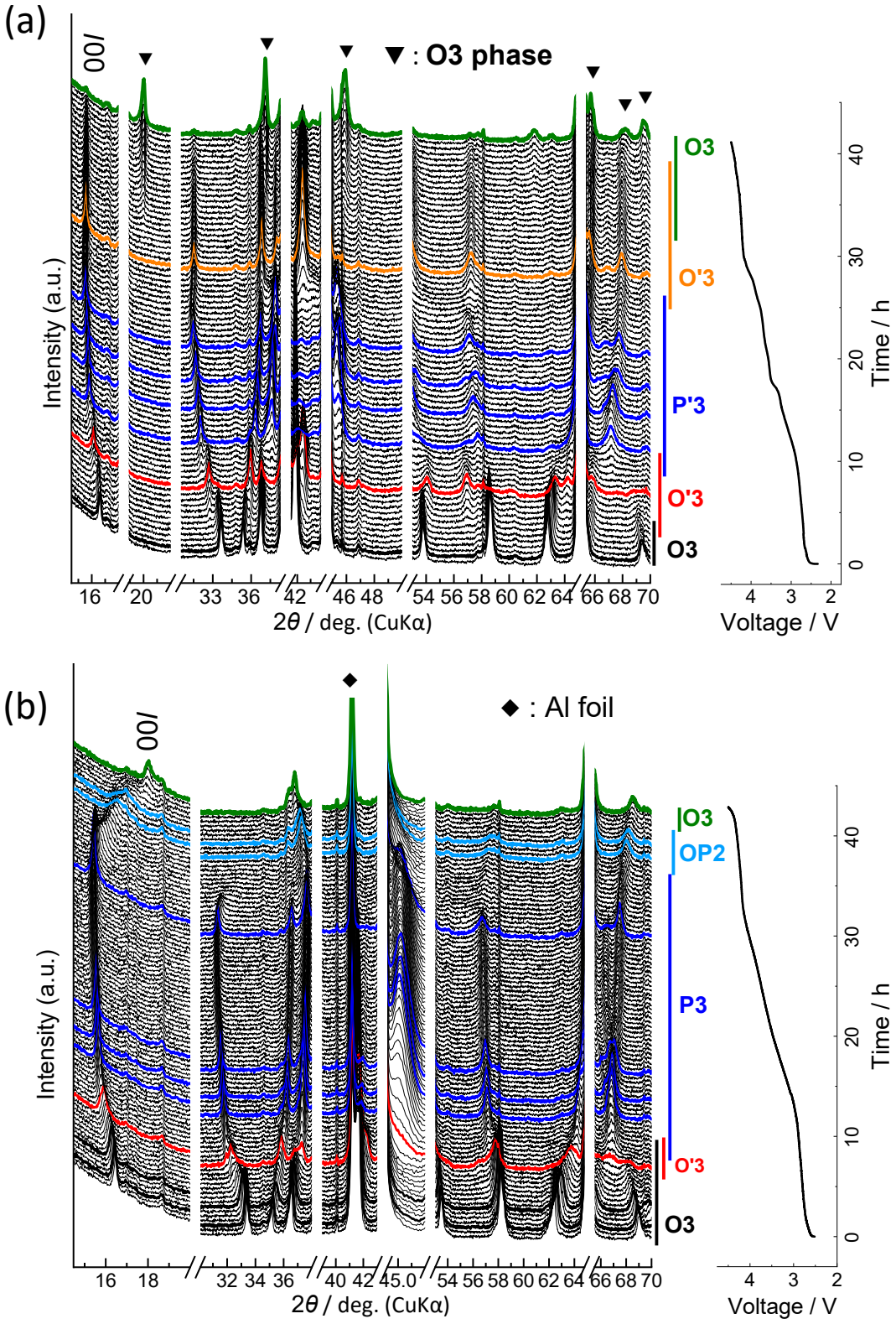

Figure S8 *Operando* XRD patterns of (a) Non-sub and (b) Mg-Ti-sub during initial charging to 4.5 V. Magnified patterns of the thick lines are shown in Fig. S9 with the peak intensities of an Al-coated Be window and an Al current collector subtracted.

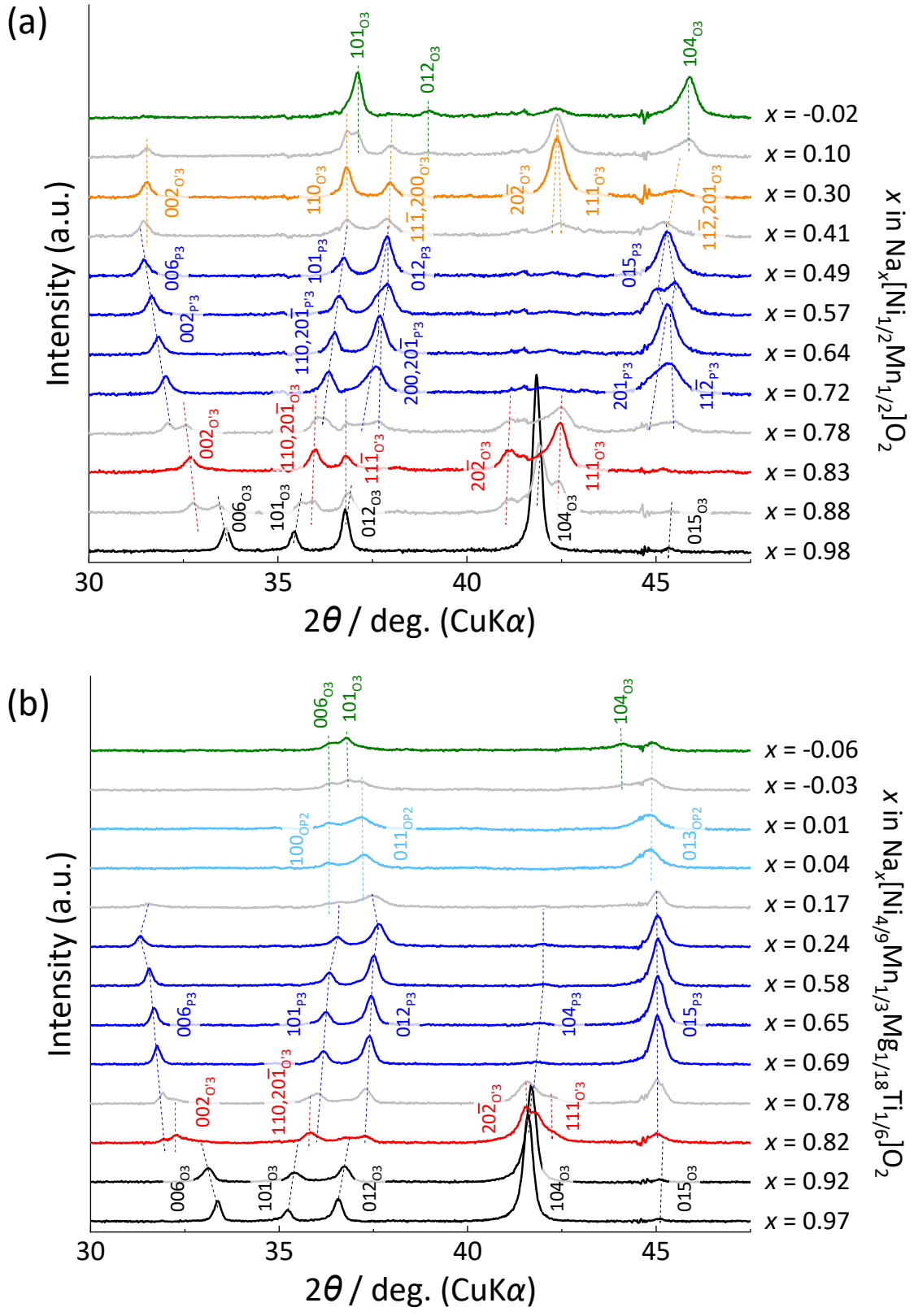

Figure S9 Selected *operando* XRD patterns of (a) Non-sub and (b) Mg-Ti-sub during initial charging to 4.5 V. The peak intensities for an Al-coated Be window and an Al current collector are subtracted from the original patterns of Fig. S8.

Table S6 Rietveld refinement results for the e*x situ* synchrotron XRD pattern of the Non-sub electrode charged to 3.35 V.

R_{wp} = 6.47%, R_e = 2.19%
Space group: $P2_1/m$
a = 4.9527(3) Å, b = 5.7081(2) Å, c = 5.8405(2) Å, β = 105.708(4)°, V = 158.95(1) Å^3
R_B = 1.12%, R_F = 0.59%

Atom	Wyckoff site	*x*	*y*	*z*	*g*	*B* / Å^2
Na1	2e	0.712(1)	1/4	0.5089(8)	0.76(1)	1.5
Na2	4f	= *x*(Na1) − 1/2	0	= *z*(Na1)	= 1/2 − 1/2**g*(Na1)	1.5
Ni1	2a	0	0	0	0.5	0.12(2)
Mn1	2a	0	0	0	0.5	= *B*(Ni1)
Ni2	2e	1/2	1/4	0.0117(6)	0.5	= *B*(Ni1)
Mn2	2e	1/2	1/4	= *z*(Ni2)	0.5	= *B*(Ni1)
O1	2e	0.878(3)	1/4	0.144(2)	1	0.66(6)
O2	2e	0.130(3)	1/4	0.827(2)	1	= *B*(O1)
O3	4f	0.386(2)	0	0.195(1)	1	= *B*(O1)

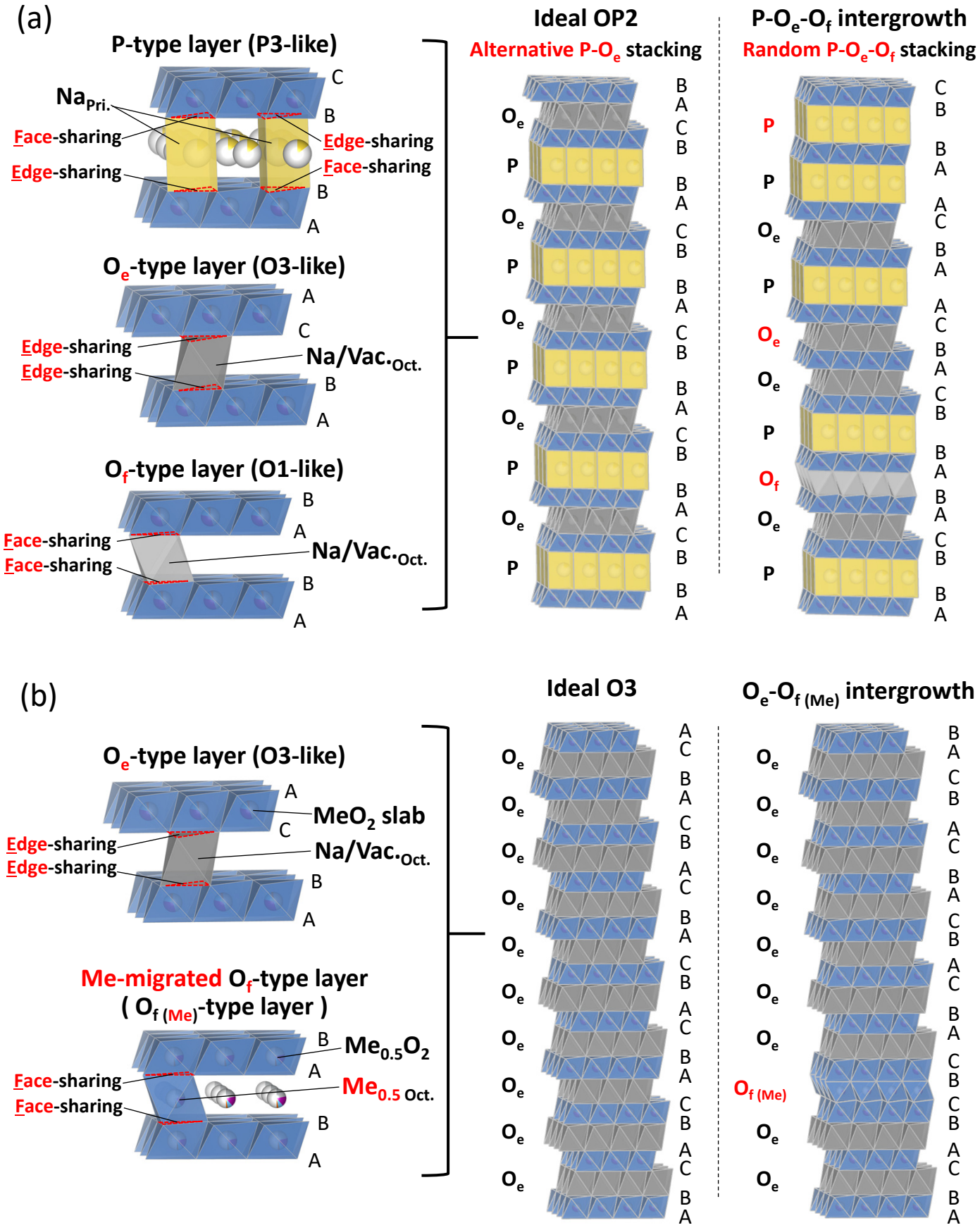

Figure S10 Schematic illustrations of structural models with stacking faults for (a) P-O_e-O_f phase and (b) O_e-$O_{f\ (Me)}$ phase and layer components.

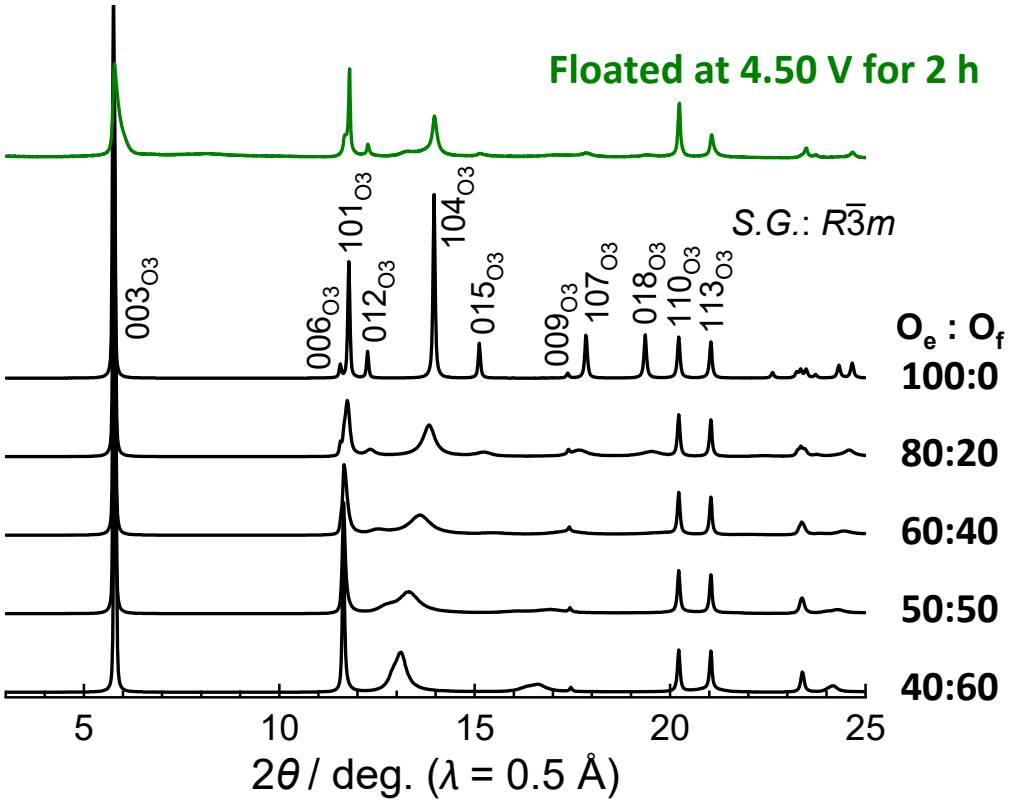

Figure S11 Simulated XRD patterns of O_e-O_f type stacking faulted structures in comparison to the observed ones in the charged state of 4.50 V.

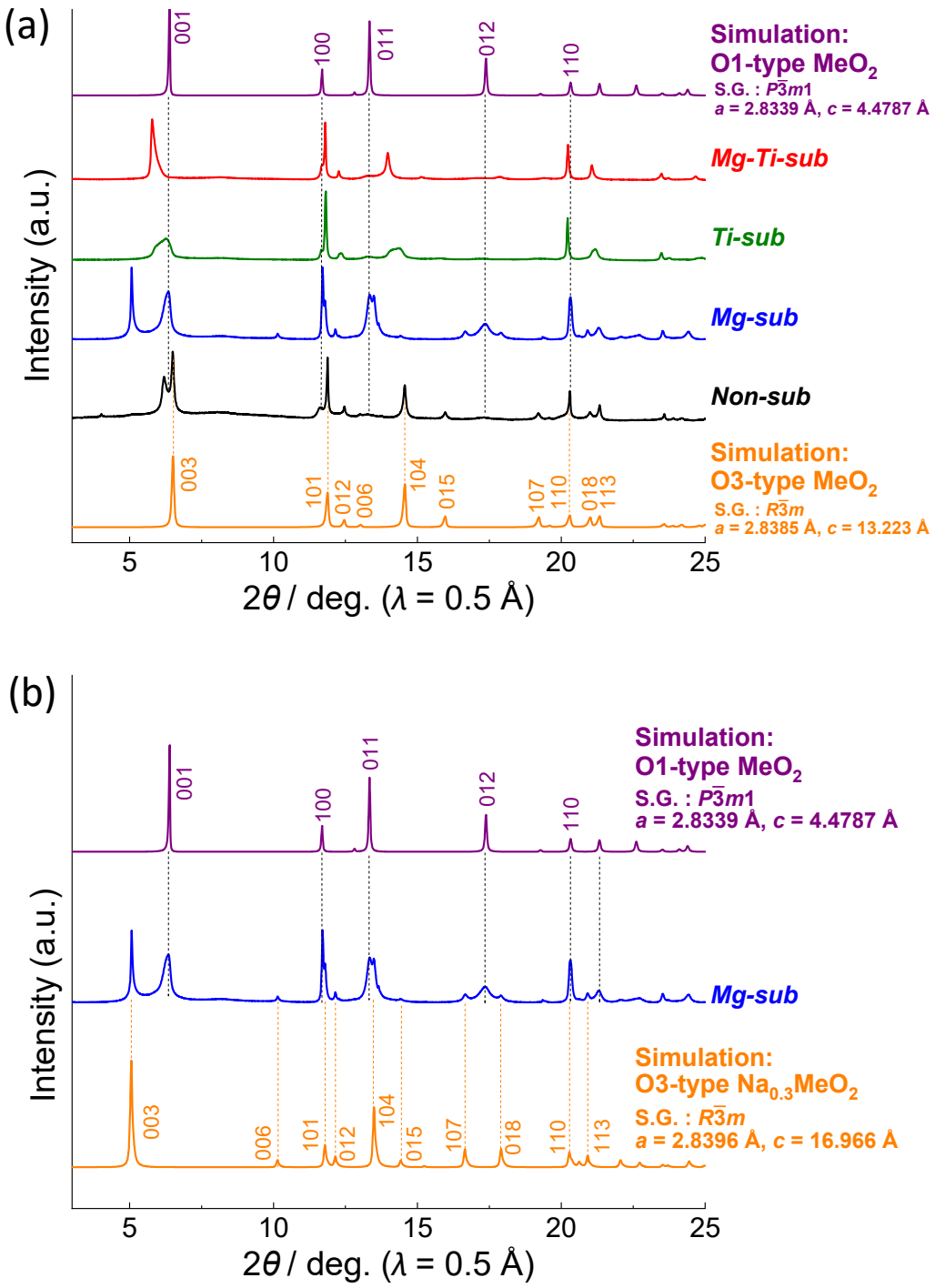

Figure S12 (a) *Ex situ* synchrotron XRD patterns of Non-sub, Mg-sub, Ti-sub, and Mg-Ti-sub electrodes after charging to 4.5 V and floating for 2 h. (b) Comparison of e*x situ* synchrotron XRD pattern for Mg-sub and with simulated patterns of O1 and O3 type structures.

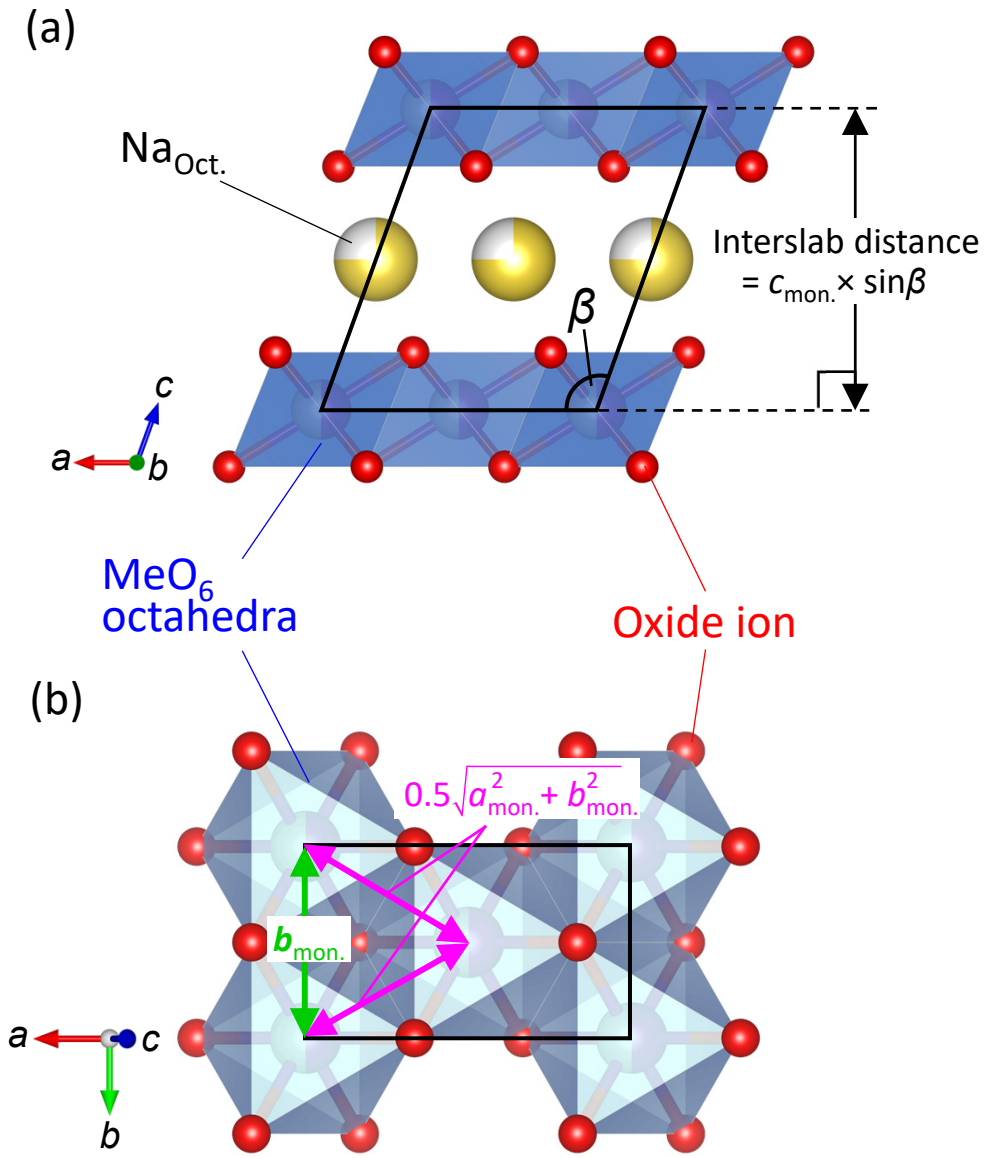

Figure S13 Schematic illustrations of a monoclinic O'3 type structure: (a) a layered structure and interslab distance and (b) an in-plane structure and Me-Me distances.